Tailored Oxygen Framework of Li4Ti5O12 Nanorods for High-Power Li Ion Battery

ARTICLE *in* JOURNAL OF PHYSICAL CHEMISTRY LETTERS · MARCH 2014

Impact Factor: 7.46 · DOI: 10.1021/jz5002924

THE JOURNAL OF PHYSICAL CHEMISTRY Letters

Letter

pubs.acs.org/JPCL

Tailored Oxygen Framework of $Li_4Ti_5O_{12}$ Nanorods for High-Power Li Ion Battery

Kyeongse Song,[†,∥] Dong-Hwa Seo,[‡,⊥,∥] Mi Ru Jo,[†] Yong-Il Kim,[§] Kisuk Kang,*[,‡] and Yong-Mook Kang*[,†]

[†]Department of Energy and Materials Engineering, Dongguk University-Seoul, 30, 1-gil, Pildong-ro, Jung-gu, Seoul 100-715, Republic of Korea

[‡]Department of Materials Science and Engineering, Research Institute of Advanced Materials, Seoul National University, Gwanak-ro 599, Gwanak-gu, Seoul 151-742, Republic of Korea

[§]Korea Research Institute of Standards and Science (KRISS), 267 Gajeong, Yuseong, Daejeon 305-340, Republic of Korea

Supporting Information

ABSTRACT: Here we designed the kinetically favored $Li_4Ti_5O_{12}$ by modifying its crystal structure to improve intrinsic Li diffusivity for high power density. Our first-principles calculations revealed that the substituted Na expanded the oxygen framework of $Li_4Ti_5O_{12}$ and facilitated Li ion diffusion in $Li_4Ti_5O_{12}$ through 3-D high-rate diffusion pathway secured by Na ions. Accordingly, we synthesized sodium-substituted $Li_4Ti_5O_{12}$ nanorods having not only a morphological merit from 1-D nanostructure engineering but also sodium substitution-induced open framework to attain ultrafast Li diffusion. The new material exhibited an outstanding cycling stability and capacity retention even at 200 times higher current density (20 C) compared with the initial condition (0.1 C).

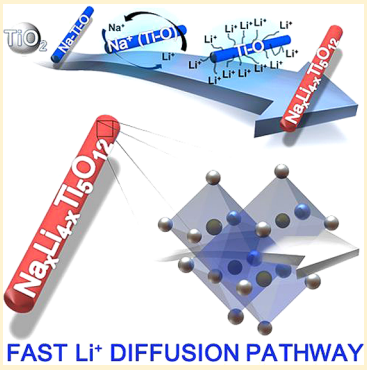

SECTION: Energy Conversion and Storage; Energy and Charge Transport

Lithium titanate spinel ($Li_4Ti_5O_{12}$) has attracted considerable attention as next-generation anode materials for high-power rechargeable lithium-ion batteries (LIBs), which do not require an SEI,[1−4] even if the safety issues related to gas evolution during charge/discharge at elevated temperatures as well as relatively low-energy density resulting from high potential around 1.55 V versus Li^+/Li still remained as serious handicaps.[5,6] The structure of spinel $Li_4Ti_5O_{12}$ ($[Li_{1+x}]_{8a}[Li_{1/3}Ti_{5/3}]_{16d}O_4$) consists of a cubic close-packed oxygen array in which Li atoms are located at both the 8a tetragonal sites and 1/6 of the 16d sites, while the remaining 5/6 of the 16d sites are occupied by titanium atoms with the space group $Fd3m$.[7,8] During the charging process, Li intercalation into the 16c sites is accompanied by Li^+ ion transfer from the 8a sites to the 16c sites, leading to the phase transition from the spinel to the rock-salt structure, in which the 8a site is empty.[9−11] In addition, $Li_4Ti_5O_{12}$ is known as "zero-strain insertion material" because the transition reaction of $Li_{4+x}Ti_5O_{12}$ ($0 \le x \le 3$) does not undergo lattice parameter change resultantly with exceptional reversibility.

To take advantage of this outstanding stability for the emerging application of high-power LIBs, the fast Li insertion/extraction into/from the $Li_{4+x}Ti_5O_{12}$ is essential to attain. Therefore, intensive research effort has been dedicated to the nanosizing and the morphology control of $Li_{4+x}Ti_5O_{12}$ to shorten Li ion diffusion length.[12−14] In details, fabrication and application of one dimensional (1-D) $Li_{4+x}Ti_5O_{12}$ such as nanowire, nanorod, nanobelt, and nanotube are of especially considerable interest due to their apparent performance improvements.[15−17] The 1-D nanostructure can give large surface-to-volume ratio, shortened Li ion diffusion length, and easily ensured e^- contact point between materials and conducting agents to facilitate the electrochemical reaction of electrode.[18,19] Therefore, 1-D nanostructured materials may well be suited for the electrodes of high-power battery applications for electric vehicles and so on. However, there has been a clear limitation to improve the kinetics of electrode materials just depending on these engineering approaches due to the accompanied disadvantages of nanomaterials.[20] Thus, we attempted to improve intrinsic Li diffusivity of $Li_{4+x}Ti_5O_{12}$ by tailoring its oxygen framework with a sodium doping. Because Li diffusion inside the electrode material tends to be sensitively determined by the interstitial spacing of the oxygen framework, building up its host structure with more open space naturally lowers the activation energy for Li ion motion. If big ions (such as Na) in the crystal structure of electrode materials could expand its oxygen framework like a pillar, Li diffusion inside the crystal structure could be significantly improved, finally realizing the kinetic enhancement as electrode. Indeed, previous first-principles study on layered cathodes has shown that the

Received: February 11, 2014
Accepted: March 24, 2014

   dx.doi.org/10.1021/jz5002924 | J. Phys. Chem. Lett. 2014, 5, 1368−1373

interspace plays an important role in determining Li mobility.[21] Also, Kang et al. reported that the lattice mismatch or lattice expansion by large ionic radius of Na^+ residues in Li-$(Ni_{0.5}Mn_{0.5})O_2$ can cause not only a better structural ordering but also a kinetic improvement due to expanded Li ion pathway.[22]

We report on the effect of sodium doping on the spinel structure of $Li_4Ti_5O_{12}$ and the correlation between the change of oxygen framework and the varied electrochemical performance. We here revealed that the sodium-substituted spinel $Li_4Ti_5O_{12}$ has more open oxygen framework and that, combined with its 3-D high-rate diffusion pathway, it results in a significant kinetic enhancement. Moreover, a very facile route will be provided for synthesizing a spinel-structured Na-doped $Li_4Ti_5O_{12}$ nanorods having not only a morphological merit from 1-D structure engineering but also sodium-substitution-induced open framework to attain ultrafast Li diffusion.

We first investigated the Li diffusion in the fully lithiated $Li_{4+x}Ti_5O_{12}$ with rock-salt-type $Li_2Ti_2O_4$ (rock-salt LTO) structure using first-principles calculation. Li ion in 16c octahedral site of rock-salt LTO migrates to a neighboring vacant 16c octahedral site through the face-shared tetrahedral site, as shown in Figure 1a. The activated state is near the center of the oxygen triangles, which exhibits the activation energy of 433 meV, as shown in Figure 1b. The intermediate tetrahedral site is weak local minimum that is still 413 meV higher than the 16c octahedral site due to narrow spacing of the oxygen framework of rock-salt LTO. To investigate the relation between the Li mobility and the spacing of the oxygen framework, we calculated the activation energies for Li migration in hypothetically expanded and contracted rock-salt LTO structures. The activation energies tend to linearly decrease with the volume change from 99 to 102% (see Figure S1 in the Supporting Information). The activation energy is 362 meV for 1% expanded structure and 609 meV for 1% contracted structure, as shown in Figure 1b. Because the Li diffusivity is inversely proportional to the exponential of the activation energy, the Li diffusivity will dramatically change with the slight volume change of rock-salt LTO structures[21,22] (Kang and Ceder 2006; Kang and Meng et al. 2006). In the transition-state theory, the diffusivity can be estimated as in eq 1

$$D = a^2\nu^*\exp(-E_{act}/k_BT) \quad (1)$$

where a is a hopping distance, ν^* is the attempt frequency, and E_{act} is the activation energy for the hopping.[21−23] Assuming that ν^* is $\sim 10^{12}$ Hz, which is generally in the range of phonon frequencies[23,24] and a is ~3 Å, the approximated diffusion constants are 4.9×10^{-11} cm^2 s^{-1} for original rock-salt LTO, 8.6×10^{-10} cm^2 s^{-1} for 1% expanded rock-salt LTO, and 5.5×10^{-14} cm^2 s^{-1} for 1% contracted rock-salt LTO at room temperature. Even 1% volume expansion could increase the Li diffusivity by one order of magnitude.

In more realistic modeling of the lattice expansion of Na doped rock-salt LTO, we tried to substitute a Na ion into one of 16c octahedral sites that were occupied by Li ions, as shown in Figure 2a. The calculated volume of $Li_{15}NaTi_{16}O_{32}$ is 0.22% larger than that of $Li_{16}Ti_{16}O_{32}$. The activation energies for the Li hopping between nearest neighbor octahedral sites (Li1 and Li2 site) of substituted Na ions and second nearest neighbor octahedral sites (Li3 and Li4 site) in (111) plane are shown in Figure 2b. In the case of the Li1−Li2 diffusion (nearest to Na ion), the activation energy was, unexpectedly, 201 meV higher than that of rock-salt LTO. It indicates that the Li ions diffuse slowly near the substituted Na ion. It is because the Li ion becomes unstable at the tetrahedral site near Na ion due to strong repulsion with face-shared Na ion, and thus the substituted Na ion can act as the point defect blocking the Li diffusion pathway. However, the activation energy for the Li migration between Li3 and Li4 site becomes much lower than not only that of rock-salt LTO but also that of 1% expanded rock-salt LTO. This is attributed to the stabilization of the intermediate tetrahedral site due to the volume expansion and the destabilization of octahedral sites (Li3 and Li4) due to the electrostatic repulsion with larger Na ion. The Li diffusivity along Li3 and Li4 sites (thick red dashed line in Figure 2a) is 2.1×10^{-8} cm^2 s^{-1}, which is over 400 times larger than that of rock-salt LTO, as shown in Figure 2c, and thus Li ions diffuse fast along this high-rate diffusion pathway. Moreover, these high-rate pathways are well-connected in rock-salt LTO due to its 3-D diffusion pathways. The Li ions can easily take a detour through 3-D high-rate pathway in the sodium-substituted rock-salt LTO, as indicated with red arrows of Figure 2a. We also confirmed that the activation energy of Li diffusion in sodium-substituted spinel $Li_4Ti_5O_{12}$ is much lower than that in the spinel $Li_4Ti_5O_{12}$, as shown in Figure S5 in the Supporting Information. Therefore, the kinetics of $Li_{4+x}Ti_5O_{12}$ as the anode material for LIBs is expected to be enhanced by the sodium substitution.

To obtain the $Li_4Ti_5O_{12}$ with kinetic enhancement, we synthesized the sodium-substituted $Li_4Ti_5O_{12}$ nanorods by ion exchange process, as shown in Figure 3a. Ion exchange process is considered to be a promising synthetic technique for the substitution of cation, which has larger ionic radius than major

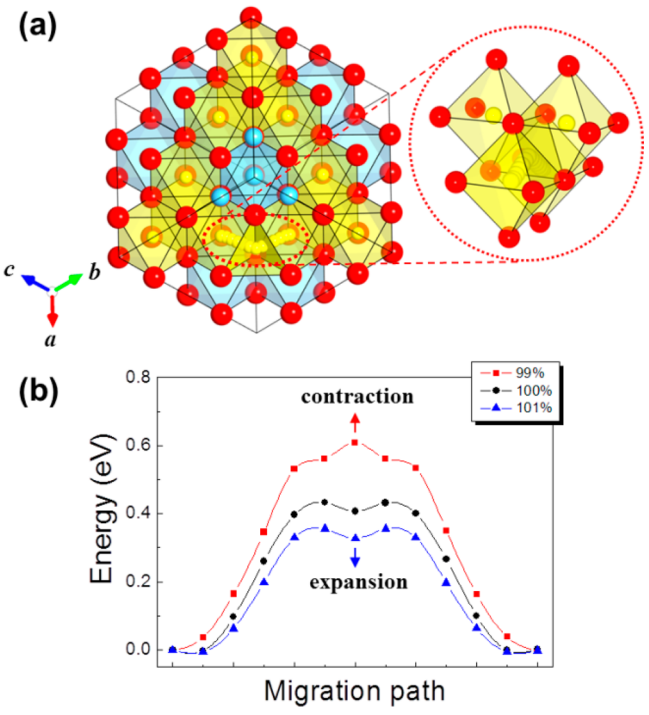

Figure 1. Schematics of the Li diffusion pathway in rock-salt LTO and its activation barrier. (a) Trajectory of the Li migration in $Li_{15}Ti_{16}O_{32}$ and (b) changes of activation energies for the Li migration with lattice expansion/contraction. The structure was drawn by VESTA software.[25]

dx.doi.org/10.1021/jz5002924 | J. Phys. Chem. Lett. 2014, 5, 1368−1373

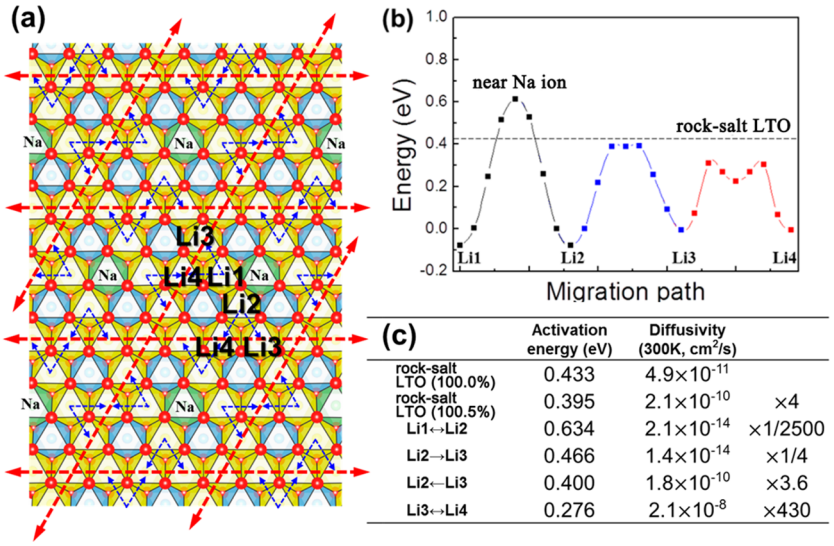

(c)

	Activation energy (eV)	Diffusivity (300K, cm^2/s)	
rock-salt LTO (100.0%)	0.433	4.9×10^{-11}	
rock-salt LTO (100.5%)	0.395	2.1×10^{-10}	×4
Li1↔Li2	0.634	2.1×10^{-14}	×1/2500
Li2→Li3	0.466	1.4×10^{-14}	×1/4
Li2←Li3	0.400	1.8×10^{-10}	×3.6
Li3↔Li4	0.276	2.1×10^{-8}	×430

Figure 2. (a) Schematics of the Li diffusion pathway in $NaLi_{14}Ti_{16}O_{32}$ in a projected *abc* plane. (b) Relative energies with respect to Li ion position along migration pathway and (c) activation energies and estimated Li diffusivity for each hopping step. Relative diffusivities compared with that of rock-salt LTO are also represented. Li1 and Li2 sites are nearest neighbor octahedral sites with the substituted sodium ion, and Li3 and Li4 sites are second nearest neighbor octahedral sites. The thick dashed lines (red) are high-rate diffusion pathways.

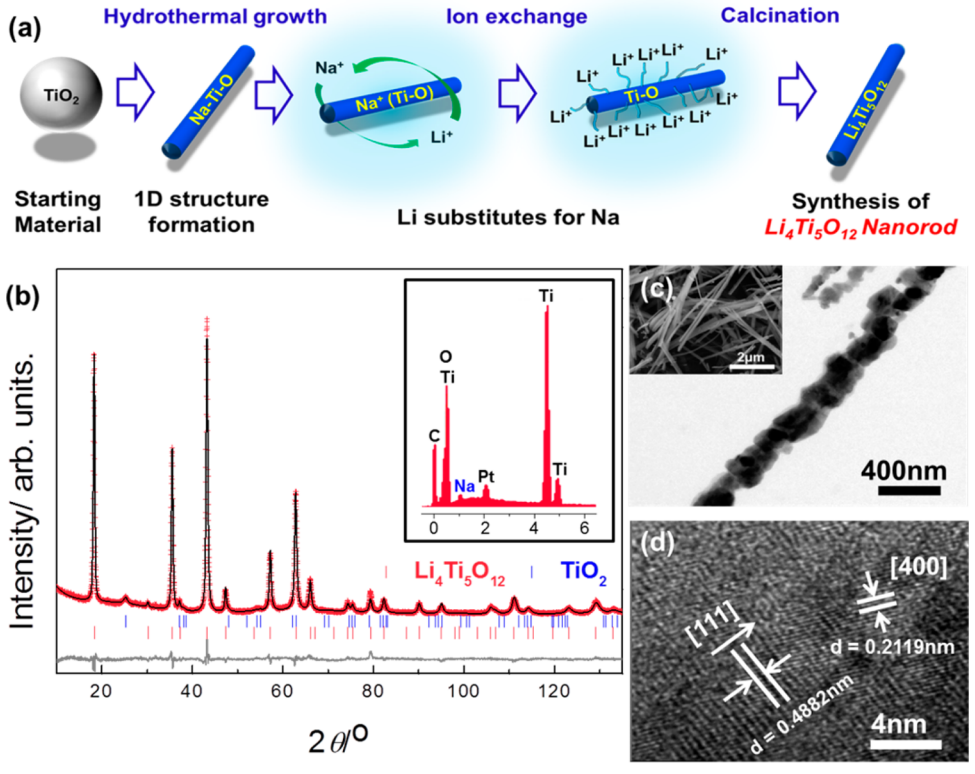

Figure 3. (a) Schematic representation for the fabrication sequence of $Na_xLi_{4-x}Ti_5O_{12}$ nanorods. Structural characterization of $Na_xLi_{4-x}Ti_5O_{12}$ nanorods. (b) Rietveld-calculated X-ray diffractograms for $Na_xLi_{4-x}Ti_5O_{12}$ nanorods (inset: EDS results of $Na_xLi_{4-x}Ti_5O_{12}$ nanorods (Pt signal come from the conducting agent)). (c) Low-resolution TEM micrograph of $Na_xLi_{4-x}Ti_5O_{12}$ nanorods. The inset shows SEM micrographs of $Na_xLi_{4-x}Ti_5O_{12}$ nanorods. (d) High-resolution TEM image of $Na_xLi_{4-x}Ti_5O_{12}$ nanorods.

cation, keeping up their nanostructures. Therefore, we successfully synthesized $Na_xLi_{4-x}Ti_5O_{12}$ nanorod by modifying the alkaline hydrothermal method including proton ion exchange process, which has been applied for synthesis of TiO_2 1-D or 2-D structure. In the first place, we made the Na−Ti−O/H−Ti−O nanorods from anatase TiO_2 nanoparticles under alkaline hydrothermal conditions and transformed the Na−Ti−O/H−Ti−O nanorods to sodium-substituted Li−Ti−O nanorods through ion exchange process between Na and Li. Finally, the synthesis of $Na_xLi_{4-x}Ti_5O_{12}$ nanorods was completed by the following calcination. The details of synthesis procedures are given in the Experimental Section in the Supporting Information.

dx.doi.org/10.1021/jz5002924 | J. Phys. Chem. Lett. 2014, 5, 1368−1373

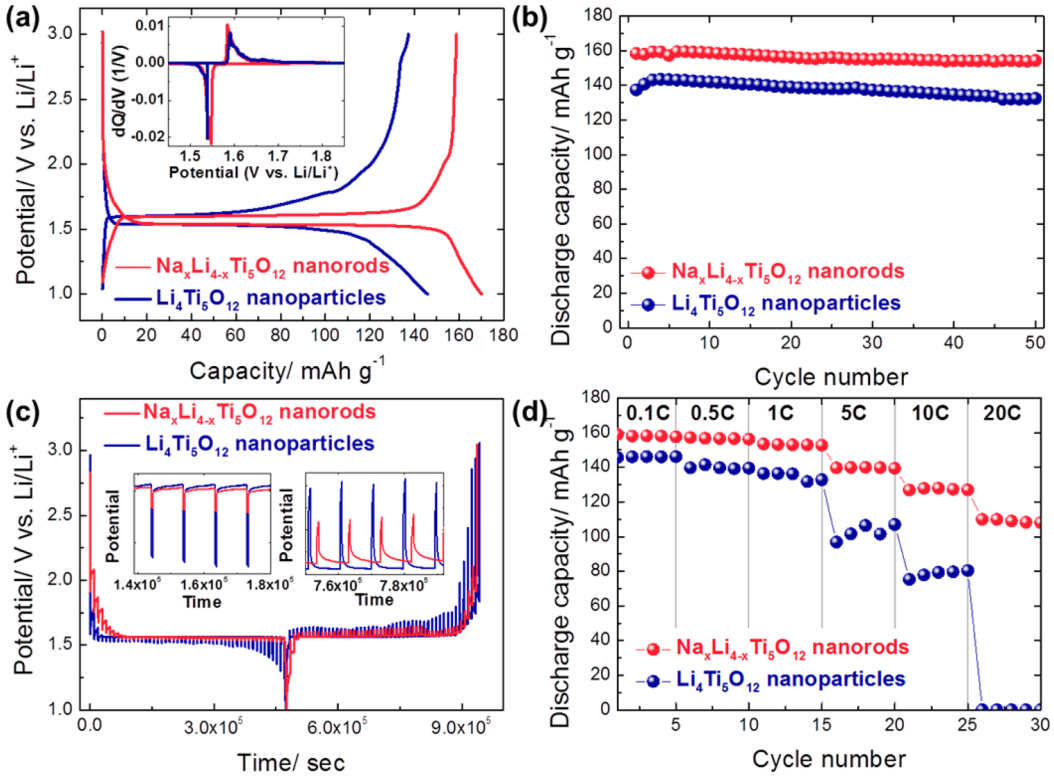

Figure 4. Electrochemical performance of $Na_xLi_{4-x}Ti_5O_{12}$ nanorods and $Li_4Ti_5O_{12}$ nanoparticles: (a) The initial galvanostatic charge/discharge curves of $Na_xLi_{4-x}Ti_5O_{12}$ nanorods and $Li_4Ti_5O_{12}$ nanoparticles at 0.1 C. (b) Cyclic performance at 0.1 C. (c) Galvanostatic intermittent titration curves showing various polarizations during lithiation or delithiation. (d) Plots of discharge retention versus cycle number at various C rates.

Energy-dispersive X-ray spectroscopy (EDS) analysis in Figure 3b (inset) shows the presence of sodium in the $Li_4Ti_5O_{12}$ nanorods. With X-ray diffraction (XRD) pattern of the $Li_4Ti_5O_{12}$ nanorods in Figure 3b, we conducted Rietveld refinement to identify the preferential site and amount of sodium as well as the related structural change. Because an initial crystal structural model is required to undertake the Rietveld refinement, $Li_4Ti_5O_{12}$ was assumed to have a cubic crystal system with a space group of $Fd\bar{3}m$. All reflection peaks of the sodium substituted $Li_4Ti_5O_{12}$ sample could not be indexed via the Pawley refinement using the lattice parameters and the space group for the cubic crystal system previously mentioned, which was used to start building the crystal structure model. Meanwhile, the other peaks could be identified by a small amount of anatase type of TiO_2 (4.34(3) %) having a $I4_1/amd$ space group. Considering the crystal structure of $Li_4Ti_5O_{12}$ and the ionic radius of Na ions, there are four kinds of possible models having different composition of sites for Na ions and Li ions in the framework of $Li_4Ti_5O_{12}$ when Na ions are substituted into $Li_4Ti_5O_{12}$. Among the possible models previously mentioned, the model in which Na ions partially occupy the tetrahedral sites (8a) for Li ions was the most stable phase as a result of first-principles calculations (see Figure S4 in the Supporting Information). Herein, the final converged weighted R factor (R_{wp}) was 8.16%, while the occupancy of Na ions for the tetrahedral sites (8a) was 0.094(7). Moreover, the lattice parameter obtained after the Rietveld refinement of sodium-substituted $Li_4Ti_5O_{12}$ is 8.363 Å, which is larger than that of standard value (8.359 Å) from JCPDS file no. 49-0207. From these results, atomic ratio of elements such as Li, Na, and Ti in $Na_xLi_{4-x}Ti_5O_{12}$ have been deduced as follows: Na/Li/Ti = 0.28:3.72:5.00. Furthermore, the measured atomic composition in $Na_xLi_{4-x}Ti_5O_{12}$ nanorod by inductively coupled plasma atomic emission spectrometry (ICP-AES) was Na/Li/Ti = (0.24 ± 0.001):(3.93 ± 0.03):(5 ± 0.03), which successfully supports our theoretical prediction and refinement results (see Figure S6 in the Supporting Information).

The inset scanning electron microscopy (SEM) image in Figure 3b clearly shows that the nanorods having ~200 nm diameter are uniformly constructed from TiO_2 nanocrystals. The morphology of the $Na_xLi_{4-x}Ti_5O_{12}$ nanorods was also confirmed by bright-field transmission electron microscopy (TEM), as shown in Figure 3c. We were able to conclusively prove that the $Na_xLi_{4-x}Ti_5O_{12}$ nanorods mainly consisted of nanosized particles, finally leading to uneven surface. The proper surface roughness obtained from this morphological characteristic of the $Na_xLi_{4-x}Ti_5O_{12}$ nanorods is expected to provide broader reaction site than the flat surface, resultantly serving as the efficient charge transport pathway from/to insulating $Li_4Ti_5O_{12}$ phases. The high-resolution (TEM) image in Figure 3d reveals that the lattice spacing is 4.882 and 2.119 Å for (111) and (400) lattice planes, respectively. This lattice spacing is well-suited to crystalline $Li_4Ti_5O_{12}$ phase on the whole but slightly increased. This lattice expansion observed by XRD and TEM analyses is in good agreement with the result of first-principles calculations, expecting sodium substitution in the oxygen framework inside $Li_4Ti_5O_{12}$.

Figure 4a shows the charge/discharge profiles of the $Na_xLi_{4-x}Ti_5O_{12}$ nanorods between 1 and 3 V at a rate of 0.1 C. The voltage profile and cycle performance of $Na_xLi_{4-x}Ti_5O_{12}$ nanorods exhibit relatively flat plateau and high initial capacity with excellent cycle performance up to 50 cycles compared with $Li_4Ti_5O_{12}$ nanoparticles (in Figure 4a,b). The first differential charge/discharge profile describes that $Li_4Ti_5O_{12}$ nanoparticles

dx.doi.org/10.1021/jz5002924 | J. Phys. Chem. Lett. 2014, 5, 1368−1373

suffer from much higher polarization as well, indicated by its larger voltage difference between Li^+ intercalation and deintercalation in the inset of Figure 4a. The smaller polarization of the $Na_xLi_{4-x}Ti_5O_{12}$ nanorods supports the fact that the $Na_xLi_{4-x}Ti_5O_{12}$ nanorods have better kinetics than the $Li_4Ti_5O_{12}$ nanoparticle due to the reduced activation barriers for facile Li^+ migration. For the detailed observation and discussion on this phenomenon, galvanostatic intermittent titration technique (GITT) curves have been obtained during the initial Li^+ intercalation/deintercalation into/from $Li_4Ti_5O_{12}$ nanoparticles and $Na_xLi_{4-x}Ti_5O_{12}$ nanorods, as shown in Figure 4c. Here the change of electrode resistances can be estimated from the disparity (polarization) between the open-circuit voltages (OCVs) and closed-circuit voltage (CCV) at different states of charge (SOC) because the resistance is directly calculated by the polarization. The two-phase reaction region (miscibility gap) in the polarization indicates that the transport properties of $Na_xLi_{4-x}Ti_5O_{12}$ nanorods are greatly enhanced compared with $Li_4Ti_5O_{12}$ nanoparticles. Finally, Figure 4d displays the plots of discharge retention versus cycle number at various C rates. It maintains a notable cycling stability even at 200 times higher current density compared with the initial condition, proving that $Na_xLi_{4-x}Ti_5O_{12}$ nanorods have noticeably enhanced kinetics compared with $Li_4Ti_5O_{12}$ nanoparticles in good accordance with our first-principles calculation results.

To enhance kinetic performance of $Li_{4+x}Ti_5O_{12}$ for high power battery applications, first, we investigated the effect of the sodium doping on the Li diffusion in the $Li_{4+x}Ti_5O_{12}$ with the state-of-the-art first-principles calculation. Then, we tried to synthesize the sodium-substituted $Li_4Ti_5O_{12}$ nanorods, which have high-rate diffusion pathways corresponding to the ideal results of first-principles calculations. The electrochemical comparison between $Na_xLi_{4-x}Ti_5O_{12}$ nanorods and $Li_4Ti_5O_{12}$ nanoparticles based on GITT measurement demonstrated that the sodium substitution into the oxygen framework of $Li_4Ti_5O_{12}$ can contribute enough to greatly enhancing Li^+ kinetics of $Li_4Ti_5O_{12}$ through the following lattice expansion, as expected by our calculation results. Moreover, its discharge capacity was close to the theoretical capacity of $Li_4Ti_5O_{12}$ (175 mAh g^{-1}), and the sodium substitution enabled $Li_4Ti_5O_{12}$ nanorods to have a promising cyclic and capacity retention even in very high rate up to 20 C.

■ ASSOCIATED CONTENT

Ⓢ Supporting Information

Experimental details, characterization, and analysis of data. This material is available free of charge via the Internet at http://pubs.acs.org.

■ AUTHOR INFORMATION

Corresponding Authors

*K.K.: E-mail: matlgen1@snu.ac.kr.

*Y.-M.K.: E-mail: dake1234@dongguk.edu.

Present Address

⊥D.-H.S.: Department of Materials Science and Engineering, Massachusetts Institute of Technology, Cambridge, Massachusetts 02139, United States.

Author Contributions

‖K.S. and D.-H.S. contributed equally.

Notes

The authors declare no competing financial interest.

■ ACKNOWLEDGMENTS

This research was supported by the Basic Science Program (no. 20090072972), the Converging Research Center Program (no. 2012K001258), and (NRF-2010-C1AAA001-0029018) through the National Research Foundation of Korea funded by the Ministry of Education, Science, and Technology. K.K. and D.-H.S. acknowledge the Human Resources Development program of the Korea Institute of Energy Technology Evaluation and Planning (KETEP) grant funded by the Korea government Ministry of Trade Industry and Energy (20124010203320). This work was supported by the Supercomputing Center/Korea Institute of Science and Technology Information with supercomputing resources including technical support (KSC-2012-C3-049). The Converging Research Center Program through the Ministry of Science, ICT and Future Planning, Korea (2013K000307) is acknowledged by Dr. Yong-Il Kim.

■ REFERENCES

(1) Borghols, W. J. H.; Wagemaker, M.; Lafont, U.; Kelder, E. M.; Mulder, F. M. Size Effects in the $Li_{4+x}Ti_5O_{12}$ Spinel. *J. Am. Chem. Soc.* **2009**, *131*, 17786−17792.

(2) Colbow, K. M.; Dahn; Haering, R. R. Structure and Electrochemistry of the Spinel Oxides $LiTi_2O_4$ and $Li_{43}Ti_{53}O_4$. *J. Power Sources* **1989**, *26*, 397−402.

(3) Ohzuku, T.; Ueda, A.; Yamamoto, N. Zero-Strain Insertion Material of $Li[Li_{1/3}Ti_{5/3}]O_4$ for Rechargeable Lithium Cells. *J. Electrochem. Soc.* **1995**, *142*, 1431−1435.

(4) Pyunll, S.; Kim, S. W.; Shin, H. C. Lithium Transport Through $Li_{1+\delta}[Ti_{2-y}Li_y]O_4$ (y=0; 1/3) Electrodes by Analysing Current Transients upon Large Potential Steps. *J. Power Sources* **1999**, *81*−*82*, 248−254.

(5) He, Y.-B.; Li, B.; Liu, M.; Zhang, C.; Lv, W.; Yang, C.; Li, J.; Du, H.; Zhang, B.; Yang, Q.-H.; et al. Gassing in $Li_4Ti_5O_{12}$-Based Batteries and its Remedy. *Sci. Rep.* **2012**, *2*, 913−921.

(6) Belharouak, I.; Koenig, G. M., Jr.; Tan, T.; Yumoto, H.; Ota, N.; Amine, K. Performance Degradation and Gassing of $Li_4Ti_5O_{12}$/$LiMn_2O_4$ Lithium-Ion Cells. *J. Electrochem. Soc.* **2012**, *159*, A1165−A1170.

(7) Ouyang, C. Y.; Zhong, Z. Y.; Lei, M. S. *Ab initio* Studies of Structural and Electronic Properties of $Li_4Ti_5O_{12}$ Spinel. *Electrochem. Commun.* **2007**, *9*, 1107−1112.

(8) Scharner, S.; Weppner, W.; Schmid-Beurmann, P. Evidence of Two-Phase Formation upon Lithium Insertion into the $Li_{1.33}Ti_{1.67}O_4$ Spinel. *J. Electrochem. Soc.* **1999**, *146*, 857−861.

(9) Lu, X.; Zhao, L.; He, X.; Xiao, R.; Gu, L.; Hu, Y.-S.; Li, H.; Wang, Z.; Duan, X.; Chen, L.; et al. Lithium Storage in $Li_4Ti_5O_{12}$ Spinel: The Full Static Picture from Electron Microscopy. *Adv. Mater.* **2012**, *24*, 3233−3238.

(10) Wilkening, M.; Iwaniak, W.; Heine, J.; Epp, V.; Kleinert, A.; Behrens, M.; Nuspl, G.; Bensch, W.; Heitjans, P. Microscopic Li Self-diffusion Parameters in the Lithiated Anode Material $Li_{4+x}Ti_5O_{12}$ ($0 \leq x \leq 3$) Measured by ^{7}Li Solid State NMR. *Phys. Chem. Chem. Phys.* **2007**, *9*, 6199−6202.

(11) Wagemaker, M.; van Eck, E. R. H.; Kentgens, A. P. M.; Mulder, F. M. Li-Ion Diffusion in the Equilibrium Nanomorphology of Spinel $Li_{4+x}Ti_5O_{12}$. *J. Phys. Chem. B* **2009**, *113*, 224−230.

(12) Jo, M. R.; Jung, Y. S.; Kang, Y.-M. Tailored $Li_4Ti_5O_{12}$ Nanofibers with Outstanding Kinetics for Lithium Rechargeable Batteries. *Nanoscale* **2012**, *4*, 6870−6875.

(13) Sorensen, E. M.; Barry, S. J.; Jung, H.-K.; Rondinelli, J. R.; Vaughey, J. T.; Poeppelmeier, K. R. Three-Dimensionally Ordered Macroporous $Li_4Ti_5O_{12}$: Effect of Wall Structure on Electrochemical Properties. *Chem. Mater.* **2006**, *18*, 482−489.

(14) Li, J.; Tanga, Z.; Zhang, Z. Controllable Formation and Electrochemical Properties of One-Dimensional Nanostructured Spinel $Li_4Ti_5O_{12}$. *Electrochem. Commun.* **2005**, *7*, 894−899.

(15) Tang, K. B.; Qian, Y. T.; Zeng, J. H.; Yang, X. G. Solvothermal Route to Semiconductor Nanowire. *Adv. Mater.* **2003**, *15*, 448−450.
(16) Seo, M. H.; Park, M.; Lee, K. T.; Kim, K.; Lim, J.; Cho, J. High Performance Ge Nanowire Anode Sheathed with Carbon for Lithium Rechargeable Batteries. *Energy Environ. Sci.* **2011**, *4*, 425−428.
(17) Hu, J. T.; Odom, T. W.; Lieber, C. M. Chemistry and Physics in One Dimension: Synthesis and Properties of Nanowires and Nanotubes. *Acc. Chem. Res.* **1999**, *32*, 435−445.
(18) Xia, Y.; Yang, P.; Sun, Y.; Wu, Y.; Mayers, B.; Gates, B.; Yin, Y.; Kim, F.; Yan, H. One-Dimensional Nanostructures: Synthesis, Characterization, and Applications. *Adv. Mater.* **2003**, *15*, 353−389.
(19) Park, M. S.; Wang, G. X.; Kang, Y.-M.; Wexler, D.; Dou, S. X.; Liu, H. K. Preparation and Electrochemical Properties of SnO_2 Nanowires for Application in Lithium-Ion Batteries. *Angew. Chem., Int. Ed.* **2007**, *46*, 750−753.
(20) Bruce, P. G.; Scrosati, B.; Tarascon, J.-M. Nanomaterials for Rechargeable Lithium Batteries. *Angew. Chem., Int. Ed.* **2008**, *47*, 2930−2946.
(21) Kang, K.; Ceder, G. Factors that Affect Li Mobility in Layered Lithium Transition Metal Oxides. *Phys. Rev. B* **2006**, *74*, 094105.
(22) Kang, K.; Meng, Y. S.; Breger, J.; Grey, C. P.; Ceder, G. First Principles Study of Li Diffusion in I-Li_2NiO_2 Structure. *Science* **2006**, *311*, 977−980.
(23) Morgan, D.; Van der Ven, A.; Ceder, G. Li Conductivity in Li_xMPO_4 (M = Mn, Fe, Co, Ni) Olivine Materials. *Electrochem. Solid State Lett.* **2004**, *7*, A30−A32.
(24) Seo, D.; Park, Y.; Kim, S.; Park, I.; Shakoor, R.; Kang, K. First-principles Study on Lithium Metal Borate Cathodes for Lithium Rechargeable Batteries. *Phys. Rev. B* **2011**, *83*, 205127.
(25) Momma, K.; Izumi, F. VESTA: a Three-Dimensional Visualization System for Electronic and Structural Analysis. *J. Appl. Crystallogr.* **2008**, *41*, 653.